

Fluorotubes as Cathodes in Lithium Electrochemical Cells

Haiqing Peng, Zhenning Gu, Jiping Yang, J. L. Zimmerman, P. A. Willis, M. J. Bronikowski, R. E. Smalley, R. H. Hauge, and J. L. Margrave*

Department of Chemistry and the Center for Nanoscale Science and Technology,
Rice University, 6100 Main Street, Houston, Texas 77005

Received July 3, 2001; Revised Manuscript Received August 24, 2001

ABSTRACT

Fluorotubes (C_2F) were prepared by fluorinating SWNTs with F_2/HF at 250 °C for 12 h and were consequently used as cathode material in a lithium electrochemical cell. The Raman and FTIR spectra of the fluorotubes were investigated before and after the cell was discharged. The discharging performance of the fluorotube/lithium electrochemical cell was studied and compared with that of a carbon monofluoride (CF_x)/lithium cell. Thermodynamic calculations using the ΔH_f° of fluorotubes and carbon monofluoride indicated that the potential of a fluorotube/lithium electrochemical cell, where the fluorotubes were made by the fluorination of armchair (10,10) SWNTs, should be 0.4 V higher than that of a carbon monofluoride/lithium cell. The experimental results support the theoretical calculations. The relation between SWNT diameter and cell potential was also investigated.

I. Introduction. Laser oven produced single-wall carbon nanotubes (SWNTs) (diameter: 1.3 nm) were fluorinated in previous work, and it was found that after fluorination of SWNTs for 12 h at 250 °C with F_2/HF , the product fluorotube formula was close to C_2F .¹ This product could be easily defluorinated back to SWNTs by sonication with hydrazine. It is believed that fluorotubes will offer new opportunities in chemistry by sidewall functionalization, cross linking, etc. For example, alkylated nanotubes were prepared by reacting fluorotubes with alkyl lithium or Grignard reagents.²

Lithium/carbon monofluoride (CF_x) batteries have long been commercial products because of their thermal stability and low self-discharge rates. Several kinds of carbon starting materials have been used, and their performance characteristics have been investigated.³ After C_{60} was discovered and fluorinated, its electrochemical properties as a cathode material were also reported.⁴ Some authors have reported the behavior of fluorinated carbon nanotubes in an electrochemical cell where the carbon nanotubes were made by decomposition of acetylene over silica-supported cobalt catalysts and fluorinated by $F_2/HF/IF_2$ at room temperature or 500 °C.⁵ Here we fluorinated SWNTs at 250 °C to make fluorotubes and used these as the cathode and lithium foil as the anode in electrochemical cells. The FTIR spectra and Raman spectra of the cathode were investigated before and after the cell was discharged. The discharge performance was

studied at room temperature and compared with a carbon monofluoride/lithium cell.

II. Experimental Details. The starting material was produced by the laser vaporization method.⁶ Metal catalysts and non-nanotube carbon were removed by a two-stage cleaning process developed by Chiang *et al.*⁷ Fluorotubes were produced by fluorinating SWNTs with a fluorine and hydrogen fluoride gas mixture (1 to 1 ratio in volume) at 250 °C for 12 h while helium gas was used as a carrier.¹ Fluorotubes were used as cathode materials, and lithium foil (Aldrich) was used as the anode in the electrochemical cell as shown in Figure 1. The diameter and thickness of the cell were 0.8 and 0.1 in., respectively. Inside the Teflon holder and stainless steel cover, lithium and fluorotubes were separated by a porous polyethylene membrane that was soaked with 1 M $LiBF_4$ in 1,2-dimethoxyethane and propylene carbonate (1 to 1 ratio in volume). $LiBF_4$ (Aldrich) was vacuum dried at 100 °C for 24 h; the 1,2-dimethoxyethane and propylene carbonate were distilled to remove water. The cell construction operations were all performed in a drybox filled with argon to prevent any effects from oxygen and moisture.

The Raman spectra of SWNTs and fluorotubes were obtained before the electrochemical cell was assembled. After the cell was discharged at room temperature, the fluorotube cathode material was collected and rinsed with methanol and vacuum dried at 70 °C overnight and then the Raman spectrum was taken. Finally, the discharged and rinsed cathode material was annealed at 800 °C for 1 h in an argon atmosphere before the Raman spectrum of the annealed material was taken. All the Raman spectra were obtained

* Corresponding author. E-mail: margrav@rice.edu; Tel: (713) 348-4813; Fax: (713) 523-8236.

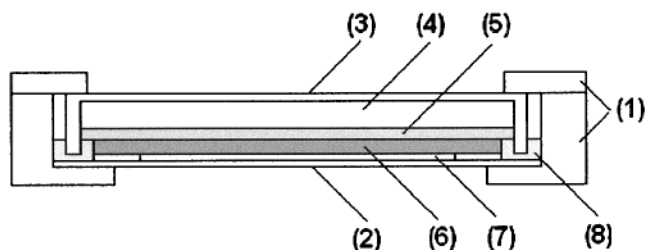


Figure 1. Schematic illustration of a lithium/fluorotube electrochemical cell. (1) Teflon holder, (2) stainless steel (cathode), (3) stainless steel (anode), (4) lithium foil, (5) porous polyethylene membrane soaked with electrolyte, (6) fluorotubes, (7) Ti current collector, (8) rubber separator.

with a Renisaw 1000 Raman system with a 780 nm wavelength laser source. The FTIR (Nexus 870) spectra of the fluorotube cathode material were also collected before and after discharging the cell.

A series of discharging experiments was performed as described by the following. Samples of fluorotubes with masses 6 mg, 20 mg, and 40 mg were dispersed in DMF (Aldrich) with the same amount of graphite powder (Aldrich, 1 to 2 μm particle size). The mixture was filtered to obtain fluorotube/graphite membranes that were oven dried at 70 $^{\circ}\text{C}$ for more than 4 h before being placed in the electrochemical cell as cathodes. A comparison between the discharge performances of carbon monofluoride (CF_x) and fluorotube cells was made. We also dispersed 20 mg fluorotubes or 20 mg CF_x (where $x = \sim 1$, MARCHEM, Houston) in DMF with 20 mg SWNTs and filtered to obtain membranes that could be placed in cells as cathodes. The use of SWNTs rather than graphite powder facilitated the formation of membranes, with comparable physical properties. The electrochemical cells with fluorotubes or CF_x were discharged across a 2 $\text{k}\Omega$ resistor load; real time voltage across the resistor was monitored and recorded by a Vernier Labpro system. HiPco (high-pressure CO) SWNTs made at Rice University with a smaller diameter than those made in laser oven process (~ 1 nm versus 1.3 nm in diameter) were fluorinated at 150 $^{\circ}\text{C}$ to obtain the C_2F formula based on weight gain and elemental analysis. The open circuit voltages of lithium electrochemical cells with CF_x , fluorinated laser oven SWNTs (L-SWNTs), and HiPco SWNTs (H-SWNTs) as cathodes were measured at various cathode loads. This was done by replacing the 2 $\text{k}\Omega$ resistor with a 200 $\text{k}\Omega$ resistor for a certain period of time after the cell had been discharged at 2 $\text{k}\Omega$ for a period of time. After recording the voltages across the 200 $\text{k}\Omega$ resistor, the system was switched back to 2 $\text{k}\Omega$ to continue the discharge. We repeated this measurement and discharge program until the cell was exhausted. By integration using the discharge curve, the open circuit voltages versus percentage of the cathode utilized were obtained and plotted. Fluorinated H-SWNTs were partially discharged, and the Raman spectra were obtained to determine if the discharge had any size dependence. A sample of 1 mg pure fluorotubes was used as cathode and discharged. The discharged fluorotubes were rinsed with methanol and water to remove the organic solvents and the electrolyte. A SEM image was obtained after drying.

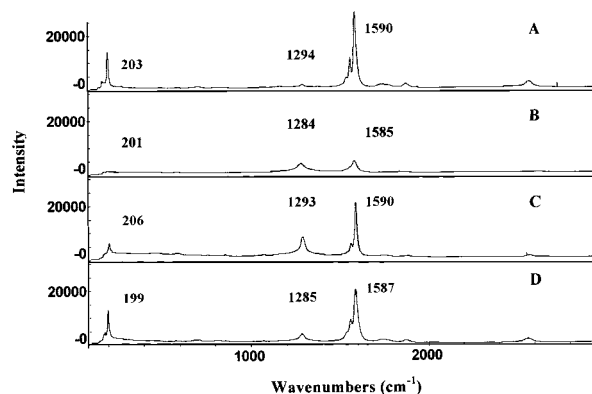


Figure 2. Raman spectra of fluorotubes (L-SWNTs) before and after discharge. (A) purified SWNTs; (B) fluorotubes; (C) after discharge; (D:) after discharge and annealing.

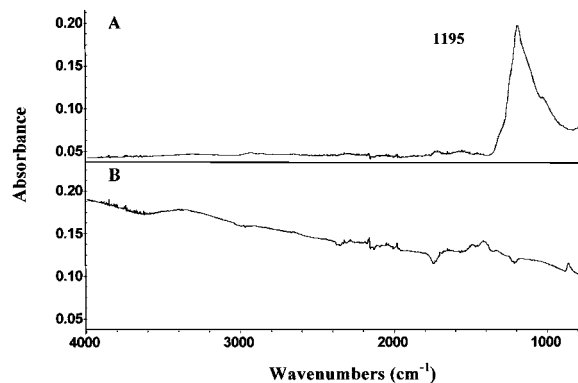


Figure 3. FTIR spectra of fluorotubes (L-SWNTs) before and after discharge. (A) fluorotubes; (B) discharged fluorotubes.

III. Discussions and Conclusions. The Raman spectra of SWNTs have been studied extensively.^{8,9,10} As Figure 2A shows, the L-SWNTs material has a strong tangential mode at 1590 cm^{-1} that is independent of nanotube diameter and A_{1g} radial breathing modes near 203 cm^{-1} that are useful in determining the distribution of nanotube diameters.⁹ Figure 2B shows the Raman spectrum for L-SWNT fluorotubes. Figure 2C shows the Raman spectrum for discharged fluorotubes, where both radial breathing and tangential modes are recovered, indicating that during the process of discharging the fluorotubes lose fluorine anions and are reduced to their original state. Equation 1 (below) represents the overall reaction.

That the 1293 cm^{-1} peak is still significant in Figure 2C suggests that the disorder caused by fluorination is not reversed by the loss of fluorine. The same phenomenon is also observed while hydrazine is used to reduce the fluorotubes.¹ As was the case for hydrazine reduction, it is seen in Figure 2D that the ~ 1293 cm^{-1} peak is significantly decreased and shifted to 1285 cm^{-1} by annealing the discharged fluorotubes at 800 $^{\circ}\text{C}$ under an argon atmosphere for 1 h. The FTIR spectra of the fluorotubes before and after the cell discharge are shown in Figure 3A and 3B. The peak at ~ 1195 cm^{-1} in Figure 3A indicates the existence of carbon–fluorine bonds. The FTIR spectrum of the discharged fluorotubes shown in Figure 3B confirmed that discharging the cell removes the C–F bonds, as indicated by the

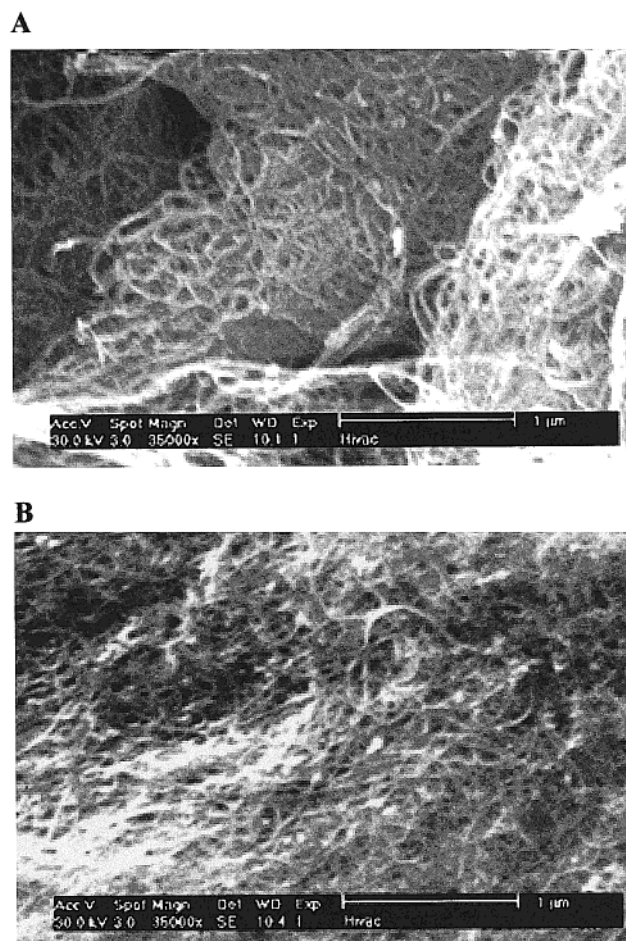


Figure 4. SEM images of fluorotubes (L-SWNTs) before and after discharge. (A) fluorotube; (B) discharged fluorotube.

disappearance of the C–F stretch. SEM images of fluorotubes before and after discharge are shown in Figure 4A and 4B. Figure 4B shows that after fluorine removal, the nanotubes ropes appear unchanged.

Electrochemical cells with 6, 20, or 40 mg fluorotubes (produced from L-SWNTs) mixed with the same amount of graphite powder as cathode materials were each discharged five times across a 2 kΩ resistance load. The respective discharging curves are shown in traces a, b, and c in Figure 5A. Traces b, b', and b'' in Figure 5A represent the discharging curves of 20 mg of fluorotubes mixed with graphite powders, without mixing with graphite power, and mixed with 20 mg L-SWNTs. The similarity between b, b', and b'' indicates that addition of graphite or SWNTs as conductive media was not necessary under our experimental conditions. The discharging curve of the cell with 20 mg CF_x mixed with the same amount of SWNTs as the cathode is shown by trace d in Figure 5A. Comparing the trace b with d indicates the fluorotube cell lasted a shorter time, consistent with the fact that the fluorine content of fluorotubes is lower than that of CF_x, while the higher voltage of the fluorotube cell indicates that the C–F bonds of fluorotubes are weaker than those of CF_x. The power discharged to reach a voltage of 1.5 V for the 20 and 40 mg fluorotube cells and the 20 mg CF_x cell are 0.024, 0.063, and 0.047

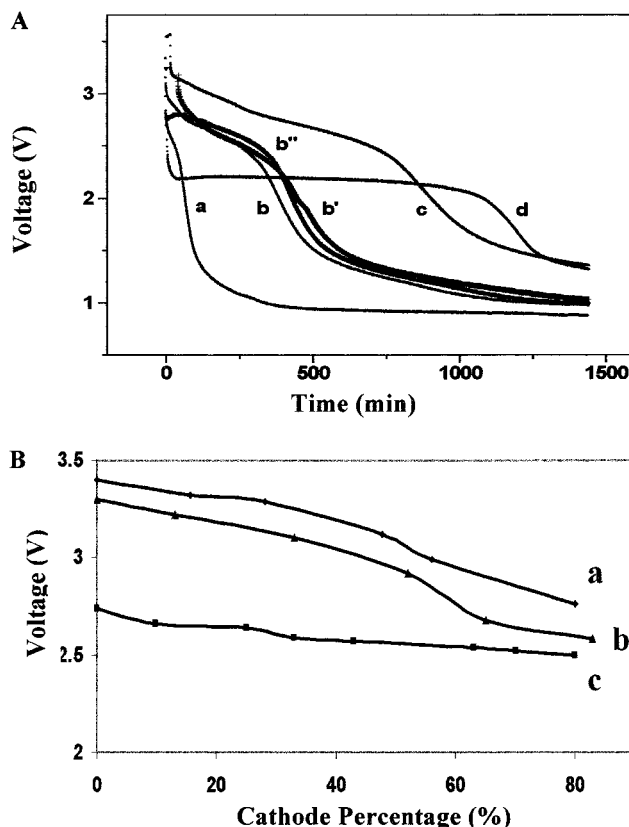


Figure 5. Discharging curves of fluorotubes (L-SWNTs) and carbon monofluoride electrochemical cell. (A) Trace a: discharging curve of 6 mg fluorotube cell at 2 kΩ; Trace b: discharging curve of 20 mg fluorotube cell at 2 kΩ; Trace b': discharging curve of 20 mg fluorotube cell (no graphite) at 2 kΩ; Trace b'': discharging curve of 20 mg fluorotubes cell at 2 kΩ; Trace c: discharging curve of 40 mg fluorotube cell at 2 kΩ; Trace d: discharging curve of 20 mg CF_x cell at 2 kΩ. In traces a, b, and c, fluorotubes were mixed with same amount of graphite as cathodes; in trace b', only fluorotubes were used; in traces b'' and d, fluorotubes and CF_x were mixed with the same amount of SWNTs. (B) Trace a: open circuit voltage of fluorinated L-SWNTs vs cathode percentage; Trace b: open circuit voltage of fluorinated H-SWNTs vs cathode percentage; Trace c: open circuit voltage of CF_x vs cathode percentage.

W*H. This corresponds to 0.0027, 0.0036, 0.0038 W*H per mg fluorine, respectively. The discharge curves for fluorotubes show two distinct slopes with the inflection point occurring when ~65–70% of the fluorine has been removed. The last ~35% fluorine appears more strongly bonded to the nanotube. This may suggest that C₂F fluorotubes are first converted to C₄F while fluorine is removed.

Wood et al. fitted the experimental heats of formation of known CF_x and obtained $\Delta H_f^\circ(\text{CF}_x) = -(44x + 3x^2)$, for $x = 1$, $\Delta H_f^\circ = -47$ kcal/mol, which was in agreement with the experimental result of -46.7 ± 1 kcal/mol.¹¹ It was also in agreement with Bettinger et al.'s computation result of -46.8 kcal/mol where carbon monofluoride was made by fluorination of a graphite sheet.¹² Bettinger et al. also investigate the heat of formation of fluorotubes. Their calculations showed that for armchair (10,10) carbon nanotubes, the heat of formation of fluorotubes (C₂F) was -35.6 kcal/mol.¹² The overall cell reactions in a fluorotube cell and in a carbon monofluoride cell are shown in eqs 1 and 2,

respectively:



Previous studies have shown that nanotubes were slightly more unstable than graphite and the difference was estimated to be 1.0 kcal/mol for (10,10) nanotubes.¹² By using ΔH_f° (fluorotubes) = −35.6 kcal/mol and ΔH_f° (carbon monofluoride) = −46.8 kcal/mol, the heat of reaction (ΔH_r) of eq 1 is 9.2 kcal/mol less than that of eq 2. If we assume that both reactions have approximately the same $T\Delta S$, then ΔG_{eq1} is 9.2 kcal less than ΔG_{eq2} where $\Delta G = \Delta H - T\Delta S$, then using $E = -\Delta G/nF$, we obtain

$$E_{\text{eq1}} - E_{\text{eq2}} = (\Delta G_{\text{eq2}} - \Delta G_{\text{eq1}})/nF \quad (3)$$

This equation suggested that the voltage of the fluorotube cell will be 0.40 V higher than that of a carbon monofluoride (CF_x) cell. This assumes that the fluorotubes (C_2F) were produced from (10,10) armchair nanotubes. The diameter of a (10,10) armchair SWNT is 1.3 nm, which is similar to the diameter of L-SWNT. In Figure 5B, traces a, b, and c represent fluorinated L-SWNTs, H-SWNTs, and carbon monofluoride cells, respectively. The voltage of the fluorotube (L-SWNT) cell is ~0.7 V higher than that of carbon monofluoride cell and its discharge curve slope is steeper. The voltages were obtained across 200 k Ω resistors while the cells were stepwise discharged at 2 k Ω . At high resistance, we believe that the voltages obtained are very close to the open circuit voltages that represent the theoretical cell potential. That the voltage of fluorinated L-SWNTs cell was ~0.7 V higher than that of the CF_x cell is in reasonable agreement with the theoretical value of 0.40 V. It is also worth noting that the cell of fluorinated L-SWNTs has a 0.10 V higher potential than the cell of fluorinated H-SWNTs. It is known that HiPco tubes have a smaller average diameter, similar to that of (8,8) tubes. For (8,8) tubes, the heat of formation in terms of C_2F is calculated as −37.5 kcal/mol, 1.9 kcal/mol lower than (10,10) tubes.¹² This suggested that the cell voltage of fluorinated L-SWNTs will be ~0.08 V higher than the cell voltage of fluorinated H-SWNTs. This is consistent with the difference between traces a and b in Figure 5B. It is interesting to note that during discharging the potential of the cell drops more rapidly for the fluorotube cell than for the carbon monofluoride cell. At 80% discharge, a change of 0.7 V has occurred for the fluorotube system as compared to 0.2 V for the carbon monofluoride system. This indicates that the average apparent carbon–fluorine bond energy increases as the system is discharged. A 0.7 V change indicates a bond energy change of 16 kcal/mol. A change in apparent bond energy would occur if the larger diameter fluorotubes are selectively defluorinated before the small diameter tubes. However, based on a calculation of bond energy versus tube diameter, one expects a change of 0.2 V rather than 0.7 V. Thus we suggest that the large change is due to a carbon–fluorine bond energy dependence on the

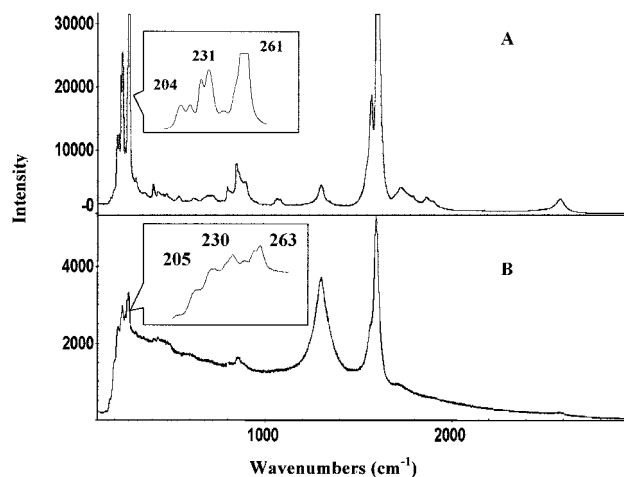


Figure 6. (A) Raman spectrum of the HiPco SWNTs. (B) Raman spectrum of the partially discharged fluorinated HiPco SWNTs.

extent of sidewall fluorination. This suggests that carbon–fluorine bonds are the strongest when the nanotube is only slightly fluorinated. To test for the question of diameter-selective defluorination, we partially discharged a fluorinated H-SWNT cell. Raman spectra of the partially discharged sample are compared to the initial unfluorinated sample in Figure 6. The breathing mode region (150–300 cm^{-1}) includes very similar relative intensities for the various peaks. This indicates that diameter selective defluorination is not occurring and supports the suggestion that carbon fluorine bond energies are dependent on the extent of sidewall fluorination. This is also in agreement with the theoretical calculation result that fluorinated nanotubes have several kinds of isomers with different stabilities.¹³

Finally, we want to point out that although we obtained higher cell potentials from fluorotubes than from carbon monofluoride, we do not intend to claim that fluorinated SWNTs are superior to carbon monofluoride as cathodes in lithium electrochemical cells. Fluorotubes cost more and have lower fluorine content. But it is very interesting to measure the cell potential difference when the fluorinated sheet-like graphite or fluorinated roll-like SWNT cathodes are used. Obviously the difference arises from the shapes of the cathode materials. Furthermore, we have found that the cell potential is diameter dependent when we compare the fluorinated L-SWNTs and H-SWNTs cathodes, and this result is in agreement with the thermodynamic calculations. This conventional electrochemical method can offer quantitative comparisons between well-defined nanostructures.

Acknowledgment. We thank NASA, NSF, the Texas Advanced Technology Program, the Robert A. Welch Foundation, and Mar. Chem, Inc. for their financial support of this research. We thank Professor Wilson for his suggestions about this research, and we also thank Professor Scuseria and Dr. Bettinger for making their fluorotube thermodynamic data available.

References

- (1) Mickelson, E. T.; Huffman, C. B.; Rinzler, A. G.; Smalley, R. E.; Hauge, R. H.; Margrave, J. L. *Chem. Phys. Lett.* **1998**, 296, 188–194.
- (2) Boul, P. J.; Liu, J.; Mickelson, E. T.; Huffman, C. B.; Erison, L. M.; Chiang, I. W.; Smith, K.; Colbert, D. T.; Hauge, R. H.; Margrave, J. L.; Smalley, R. E. *Chem. Phys. Lett.* **1999**, 310, 367–372.
- (3) Akiyoshi Morita, Takashi Iijima, Takabumi Fujii and Hiomichi Ogawa, *J. Power Source* **1980**, 5, 111–115.
- (4) Okino, F.; Liu, N.; Kawasaki, S.; Touhara, H. *Fullerenes* **3**, 191–208.
- (5) Hamwi, A.; Gendraud, P.; Gaucher, H.; Bonnamy, S.; Beguin, F. *Mol. Cryst. Liq. Cryst.* **1998**, 310, 185–190.
- (6) Guo, T.; Nikolaev, P.; Thess, A.; Colbert, D. T.; Smalley, R. E. *Chem. Phys. Lett.* **1995**, 243, 49.
- (7) Chiang, I. W.; Brinson, B. E.; Smalley, R. E.; Margrave, J. L.; Hauge, R. H. *J. Phys. Chem. B* **2001**, 105 (6), 1157–1161.
- (8) Rao, A. M.; Richter, E.; Bandow, S.; Chase, B.; Eklund, P. C.; Williams, K. A.; Fang, S.; Subbaswamy, K. R.; Menon, M.; Thess, A.; Smalley, R. E.; Dresselhaus, G.; Dresselhaus, M. S. *Science* **1997**, 275, 187–191.
- (9) Andreoni, W. *The Physics of Fullerene-Based and Fullerene-Related Material*; Kluwer Academic Publishers: Dordrecht, 2000.
- (10) Thess, A.; Lee, R.; Nikolaev, P.; Dai, H.; Petit, P.; Robert, J.; Xu, C.; Lee, Y. H.; Kim, S. G.; Rinzler, A. G.; Colbert, D. T.; Scuseria, G. E.; Tománek, D.; Fischer, J. E.; Smalley, R. E. *Science* **1996**, 273, 483–487.
- (11) Wood, J. L.; Badachhpe, R. B.; Lagow, R. J.; Margrave, J. L. *J. Phys. Chem.* **1969**, 73, 3139.
- (12) Bettinger, H. F.; Kudin, K. N.; Scuseria, G. E., submitted to *J. Am. Chem. Soc.*
- (13) Kudin, K. N.; Bettinger, H. F.; Scuseria, G. E. *Phys. Rev. B* **2001**, 63, 045413.

NL010053U